Supporting Information

Uncovering the roles of oxygen vacancy on cation migration in lithium excess layered oxides

Danna Qian[1], Bo Xu[2], Miaofang Chi[3] and Ying Shirley Meng[1*]

1. Department of NanoEngineering, University of California San Diego, La Jolla, CA 92093

2. Department of Materials Science and Engineering, Massachusetts Institute of Technology, Cambridge, MA, 02139

3. Center for Nanophase Materials Sciences, Oak Ridge National Laboratory, Oak Ridge, TN, 37831

SI1. STEM/EELS experimental details

Electron Microscopy work was carried out on a Cs-corrected FEI Titan 80/300-kV TEM/STEM microscope equipped with a Gatan Image Filter Quantum-865. All STEM images and EELS spectra were acquired at 300 kV and with a beam size of ~0.7Å. EELS spectra shown in this work were acquired from a square area of ~0.5*0.5 nm with an acquisition time of 3 seconds and a collection angle of 35mrad. HAADF images were obtained with a convergence angle of 30mrad and a large inner collection angle of 65mrad. Images acquired by an HAADF detector with a small convergence angle and a relative large inner collection angle are also called "Z-contrast" images, where the contrast is proportional to $Z^{1.7}$.[1, 2] In atomic resolution Z-contrast images, the contrast of the atomic columns thus can be used to differentiate different elements and provide atomic-structural information.

To minimize possible electron beam irradiation effects, EELS and HAADF figures presented in this work were acquired from areas without pre-beam irradiation.

SI2. Computation details

First principles calculations were performed in the spin-polarized GGA+U approximations to the Density Functional Theory (DFT). Core electron states were represented by the projector augumented-wave method[3] as implemented in the Vienna ab initio simulation package (VASP).[4-6] The Perdew-Burke-Ernzerhof[7] exchange correlation and a plane wave representation for the wavefunction with a cutoff energy of 450eV were used. The Brillouin zone was sampled with a dense k-points mesh by Gamma packing. The four-layered supercell composed of 12 formula units of $Li[Ni_{1/4}Li_{1/6}Mn_{7/12}]O_2$ used in previous work is used again to obtain the trend of oxygen vacancy formation energies. The atomic positions and cell parameters are fully relaxed to obtain

total energy and optimized cell structure. To obtain the accurate electronic structures, a static self-consistent calculation is run, followed by a non-self-consistent calculation using the calculated charge densities from the first step. The cell volume is fixed with internal relaxation of the ions in the second step calculation. The Hubbard U correction was introduced to describe the effect of localized d electrons of transition metal ions. The applied effective U value given to Mn ions is 5eV and to Ni ions is 5.96eV.[8]

A new supercell composed of 24 formula units by doubling previous supercell along the c direction is used to investigate Ni diffusion mechanisms. Nudged Elastic Band (NEB) method is used to find the minimum energy path and the energy barrier for Ni diffusion inside the materials. All models are established as bulk materials, and no oxygen diffusion is considered in this work.

To calculate formation energies of oxygen vacancy in $Li_xNi_{1/4}Mn_{7/12}O_2$ bulk, both types of supercells were used for investigations and only one vacancy was created in each cell. This is equivalent to oxygen vacancy concentration between 2% to 4%, which satisfies the dilute defect conditions. Following two equations were used to calculate the formation energy of oxygen vacancies in $Li_xNi_{1/4}Mn_{7/12}O_2$:

$$E_{fov} = E\left(Li_nNi_3Mn_7O_{23}\right) + 1/2\,E\left(O_2\right) - E\left(Li_nNi_3Mn_7O_{24}\right) \quad (1)$$

and

$$E_{fov} = E\left(Li_mNi_6Mn_{14}O_{47}\right) + 1/2\,E\left(O_2\right) - E\left(Li_mNi_6Mn_{14}O_{48}\right) \quad (2)$$

where $E(O_2)$ is the calculated energy of the oxygen gas plus a 1.36 eV correction according to previous reports [9].

SI3. Ni diffusion barriers with oxygen vacancies in different positions at $Li_{15/28}Ni_{1/4}Mn_{7/12}O_2$

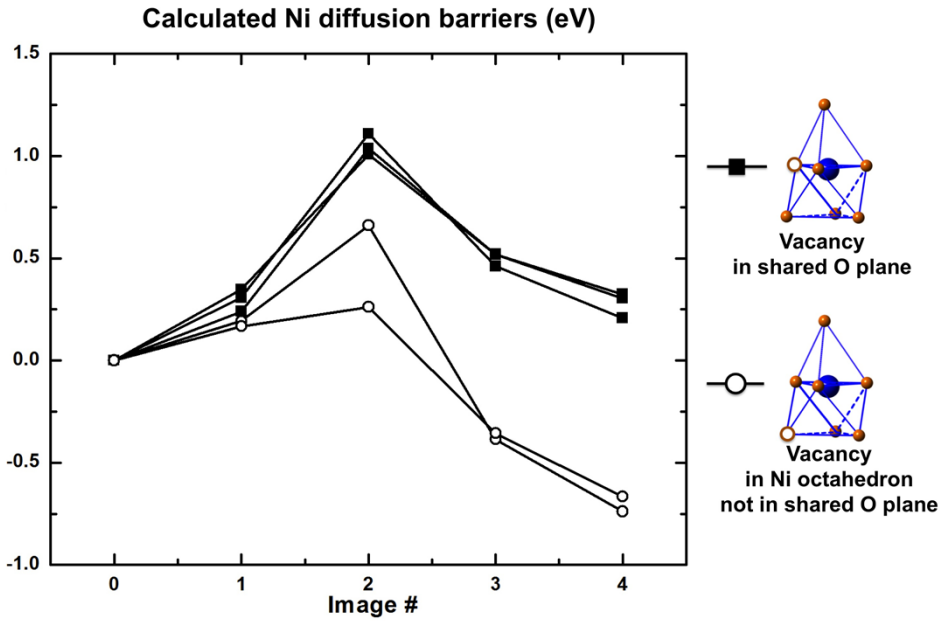

SI4. Neighboring TM valence change after introduction of oxygen vacancy at $Li_{20/28}Ni_{1/4}Mn_{7/12}O_2$

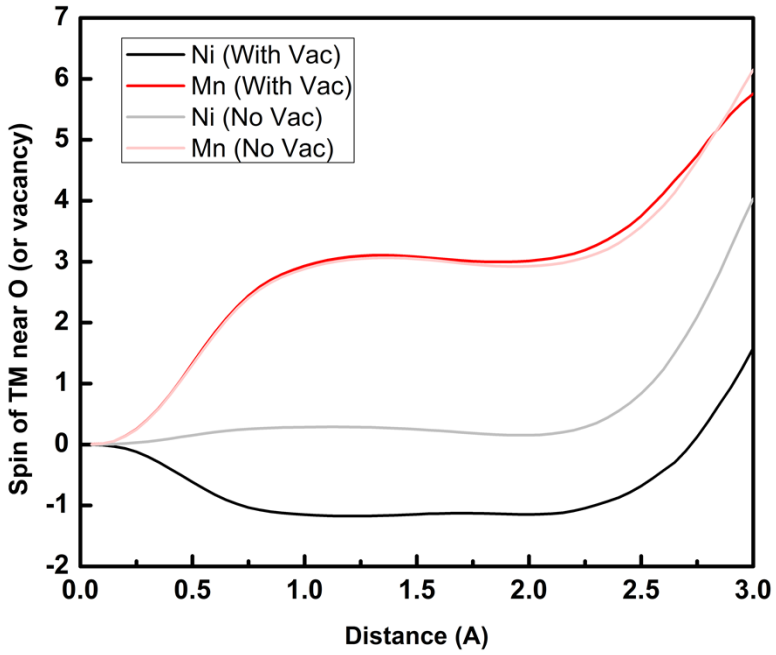

Mn does not change valence, while Ni is being reduced.

SI5. Mn diffusion barriers with oxygen vacancies in different positions at $Li_{20/28}Ni_{1/4}Mn_{7/12}O_2$

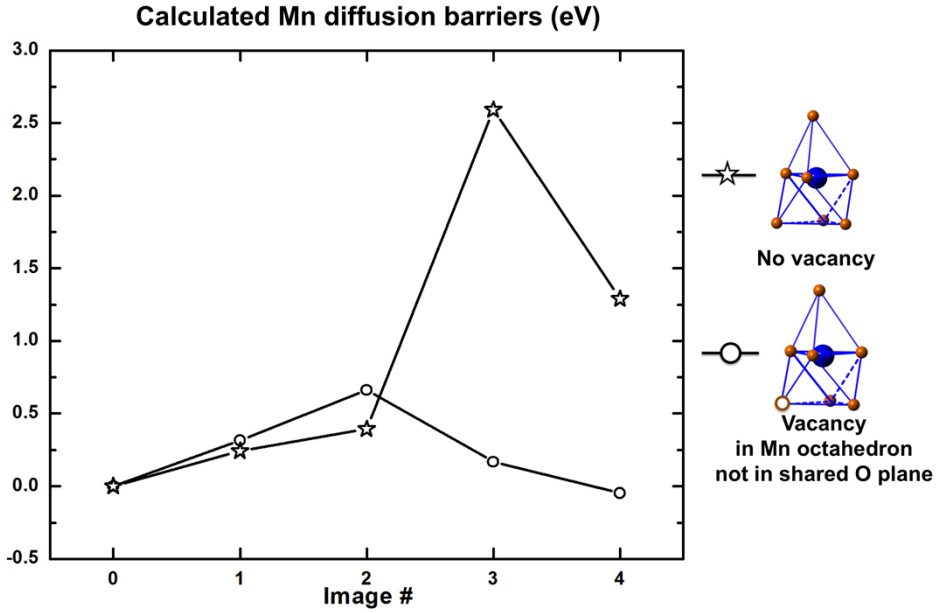

SI6. Synthesis and sample preparation experimental details

Detailed Synthesis can be found in previous publications. [10]

1. S. J. Pennycook, *Ultramicroscopy*, 1989, **30**, 58-69.
2. E. M. James and N. D. Browning, *Ultramicroscopy*, 1999, **78**, 125-139.
3. G. Kresse and D. Joubert, *Phys Rev B*, 1999, **59**, 1758-1775.
4. G. Kresse and J. Furthmuller, *Comp Mater Sci*, 1996, **6**, 15-50.
5. G. Kresse and J. Furthmuller, *Phys Rev B*, 1996, **54**, 11169-11186.
6. G. Kresse and J. Hafner, *Phys Rev B*, 1994, **49**, 14251-14269.
7. J. P. Perdew, K. Burke and Y. Wang, *Physical Review B*, 1996, **54**, 16533-16539.
8. Y. Hinuma, Y. S. Meng, K. S. Kang and G. Ceder, *Chem. Mater.*, 2007, **19**, 1790-1800.
9. L. Wang, T. Maxisch and G. Ceder, *Chem. Mater.*, 2007, **19**, 543-552.
10. H. Liu, C. R. Fell, K. An, L. Cai and Y. S. Meng, *J Power Sources*, 2013, **240**, 772-778.